

Modelling the H Lyman lines in evolved late-type stars

S. A. Sim^{*}

Department of Physics (Theoretical Physics), University of Oxford, 1 Keble Road, Oxford, OX1 3NP, UK

26 April 2001

ABSTRACT

The importance of Partial Redistribution (PRD) in the modelling of the Lyman α and Lyman β emission lines of hydrogen in stellar atmospheres is examined using simple atmospheric models of a range of late-type stars. These models represent the sub-giant Procyon (F5 IV-V), and the two giants β Gem (K0 III) and α Tau (K5 III). These stars are selected to span a wide range of surface gravities: $1.25 < \log g < 4.00$. The calculations are performed using the computer code MULTI (Carlsson 1986) with the modifications made by Hubeny & Lites (1995). It is found that PRD effects are highly significant, both in the direct prediction of the Lyman line profiles and in the application of hydrostatic equilibrium (HSE) to calculate the atmospheric electron density in static atmospheric models.

Key words: line: formation – line: profiles – radiative transfer – stars: chromospheres – stars: late-type

1 INTRODUCTION

The modelling of the Lyman lines of hydrogen is extremely important for the study of stellar atmospheres. The Lyman α line is the strongest single line in the ultraviolet spectra of cool stars and represents a significant energy loss mechanism from the high chromosphere and low transition region in most stars. The strength and width of the Lyman lines, particularly Lyman α and Lyman β , is such that they are important sources for fluorescence in the lines of other elements (Jordan & Judge 1984). This fluorescence is of particular importance in low gravity stars such as α Tau (McMurry, Jordan & Carpenter 1999).

Unfortunately, the Lyman lines are difficult to model since the extreme optical thickness of the lines and the low electron densities in the region of line formation makes the treatment of photon scattering very important. The assumption of complete (frequency) redistribution (CRD), which is often used in the modelling of the lines of other atomic species, is unacceptable because most scattering events in a transition such as Lyman α are coherent (in a giant star such as β Gem in a region where the electron temperature $T_e \sim 10^4$ K and the electron density $n_e \sim 10^9 \text{ cm}^{-3}$, only $\sim 10^{-4}$ of the scattering events are incoherent). This coherence leads to a correlation between the absorbed and emitted frequencies in a scattering event and so introduces an explicit coupling of the radiation field at different frequencies. This significantly complicates the problem that is to be solved. Thus scattering in these lines must be mod-

elled using the more complete theory of partial (frequency) redistribution (PRD).

Linsky (1985) gives a review of the work on PRD in stellar atmospheres. Early work on the Lyman α line in the solar chromosphere gave clear indications that PRD effects would be very important (Milkey & Mihalas 1973). However, the treatment of Milkey & Mihalas (1973) is not entirely satisfactory because it is based on the redistribution function theory of Omont, Smith & Cooper (1972). This redistribution function is widely used in the study of PRD in lines of Ca II and Mg II, but is not suitable for hydrogen because it assumes that the coherence fraction is frequency independent. However, the incoherence fraction is only frequency independent in the so-called *Impact Limit* of collisional broadening which is valid only in the very core of Lyman α . An adequate treatment of the line wings requires a more sophisticated atomic theory (under the conditions that exist in a giant star such as β Gem the *Impact Limit* is only valid for wavelength differences from line centre of $\leq 10^{-4}$ Å). Such a theory exists in the form of the Unified Theory of Collisions (Smith, Cooper & Vidal 1969). This theory is developed by Vidal, Cooper & Smith (1970) and specifically used to study hydrogen in stellar atmospheres by Yelnik et al. (1981) and Cooper, Ballagh & Hubeny (1989). An alternative theory of collisional broadening is discussed by Smith, Cooper & Roszman (1973).

The application of the Unified Theory in the study of PRD in hydrogen has been carried out by several authors. Basri et al. (1979) used a Unified Theory treatment of both ion and electron collisions to compute a Lyman α profile to compare with solar observations. Their calculations were

^{*} E-mail: sim@thphys.ox.ac.uk

based on the solar model of Vernazza, Avrett & Loeser (1973) which they modified to obtain close agreement with the observed profile. In their extensive study of solar chromospheric modelling, Vernazza, Avrett & Loeser (1981) also performed PRD calculations for hydrogen. In that paper, the authors experimented by setting different maximum coherence fractions and they found that enforcing a maximum coherence fraction of 98 per cent gave the best agreement with the observed data. However, they gave no physical reason why the incoherence fraction should be larger than the theoretical prediction. Luttermoser & Johnson (1992) use a PRD treatment of the Lyman α line when considering their joint photospheric/chromospheric models of the stars γ Her and TX Psc. They find that a PRD treatment of hydrogen (compared to a CRD treatment) makes a significant difference to the proton density in certain parts of their atmospheric models and is therefore significant to the ionization balance in hydrogen. Uitenbroek (1989) introduced PRD to the radiative transfer code MULTI, which in its original form is discussed by Carlsson (1986) and Scharmer & Carlsson (1985a,b). The treatment of PRD used by Uitenbroek (1989) was based on *Impact Theory* and is suitable for the Ca II H and K lines but not for hydrogen. More recently, Hubeny & Lites (1995) modified the MULTI code extensively so that it could include the frequency dependent coherence fraction required for hydrogen. They discussed the modifications to the code and the theory behind them and also successfully applied their code to the solar chromospheric model C of Vernazza et al. (1981).

The purpose of this paper is to present the results of applying the version of MULTI written by Hubeny & Lites (1995) to models of stars other than the Sun, so that PRD effects can be investigated in lower surface gravity and their importance to the modelling techniques can be studied. Several limitations remain in the approach used by Hubeny & Lites (1995) and these remain in the work here. The primary limitation of the computer code is that it implements an angle averaged redistribution function. This means that it can only be applied realistically to a static atmospheric model and so all the models discussed here are static and contain no net flows. There is also a minor assumption, made for computational ease, that when calculating the collisional broadening, it is assumed that the proton density is equal to the electron density. In a typical high chromosphere/transition region this assumption is reasonable and so should not be a source of significant error.

2 THEORY

The detailed theory of PRD in hydrogen is discussed by Cooper et al. (1989). The theory they describe, which is that implemented by Hubeny & Lites (1995), includes an acceptable treatment of resonant scattering in both Lyman α and Lyman β and also includes cross-redistribution from Balmer α to Lyman β . The details of the method are discussed by Hubeny & Lites (1995). A brief summary of those parts of the theory which are of particular relevance are given below.

The study of PRD requires the calculation of the redistribution function R which gives the probability that a photon of frequency ν' will be absorbed and re-emitted as a

photon of frequency ν . It is convenient to work in the rest frame of the absorbing atom (on the understanding that, at a later stage an average over a Maxwellian velocity distribution of such atoms will be performed). Thus the required quantity is

$$f(\nu')p(\nu', \nu)$$

where f is the absorption profile (which describes the probability that a photon of frequency ν' is absorbed) and p is the probability that, given an absorption at frequency ν' there is a subsequent re-emission at frequency ν .

The quantities f and p can be calculated from the quantum mechanical theory of radiation. As an example, for Lyman α they are given by

$$f_{1s2p}(\Delta\omega) = \frac{1}{\pi} \frac{\Gamma_{2p}(\Delta\omega)}{\Delta\omega^2 + \Gamma_{2p}(\Delta\omega)^2} \quad (1)$$

and

$$p_{1s2p}(\Delta\omega', \Delta\omega) = (1 - \Lambda_{1s2p}(\Delta\omega')) \delta(\Delta\omega - \Delta\omega') + \Lambda_{1s2p}(\Delta\omega') f_{1s2p}(\Delta\omega) \quad (2)$$

where $\Delta\omega$ and $\Delta\omega'$ are the angular frequencies (measured relative to line centre) of the emitted and absorbed photons, Γ_{2p} is the total half width of the 2p state and Λ_{1s2p} is the *incoherence fraction*. δ is the Dirac-delta function.

The total half width is given by

$$\Gamma_{2p}(\Delta\omega) = \gamma_{2p}(\Delta\omega) + \Gamma_{2p1s}/2 \quad (3)$$

where Γ_{2p1s} is the radiative decay rate in Lyman α and $\gamma_{2p}(\Delta\omega)$ is the half width due to collisional broadening (for clarity, other broadening mechanisms are neglected here). Expressions for $\gamma_{2p}(\Delta\omega)$ are given by Basri et al. (1979). The incoherence fraction is given by

$$\Lambda_{1s2p}(\Delta\omega) = \frac{\gamma_{2p}(\Delta\omega)}{\Gamma_{2p}(\Delta\omega)}. \quad (4)$$

The incoherence fraction is the probability that an atom will undergo an elastic collision (which randomly changes the energy and thus destroys coherence) before it decays. Thus Equation (2) means that a fraction Λ of scattering processes will undergo complete redistribution and a fraction $1 - \Lambda$ will undergo no redistribution. The incoherence fraction is clearly the physical quantity which determines the importance of PRD effects. It always lies between 0 and 1. If it is 0 then the transition in question exhibits pure Rayleigh (coherent) scattering, while if it is 1 the system displays complete redistribution (CRD). Thus PRD effects are only likely to be important for values of the incoherence fraction that are $\ll 1$.

The incoherence fraction is determined by the broadening parameter $\gamma_{2p}(\Delta\omega)$. This quantity is discussed in detail by Yelnik et al. (1981) and Cooper et al. (1989). It is obvious that $\gamma_{2p}(\Delta\omega)$ should be density dependent, since a lower density will lead to fewer collisions and hence a smaller incoherence fraction. Therefore, it is to be expected that PRD should be significantly more important in a giant star (such as β Gem which has a surface gravity of $5.6 \times 10^2 \text{ cm s}^{-2}$) than in a main sequence star like the Sun (surface gravity $2.75 \times 10^4 \text{ cm s}^{-2}$). It is for this reason that it is of particular interest to examine the trend of PRD effects in different types of star.

The treatment of the Lyman β line is further complicated by the possibility of resonant Raman scattering involving the Balmer α line. When a Balmer α photon is absorbed, exciting the $n = 3$ level, the $n = 3$ level may subsequently decay to $n = 1$ emitting a Lyman β photon. The frequency of the emitted Lyman β photon will be coupled to the frequency of the absorbed photon, unless a collision occurs to redistribute the $n = 3$ electron energy. A reliable treatment of the Lyman β line must therefore account not only for significant coherence in resonant scattering in the Lyman β line, but also for the effects of this so-called *cross redistribution* between Balmer α and Lyman β . Equations (47) to (49) in Hubeny & Lites (1995) show how cross redistribution appears in the emission coefficient of Lyman β .

An additional problem occurs in the application of the Unified Theory to hydrogen – the l -degeneracy of the energy levels means that the *Isolated Line* approximation is not valid. A more general theory is developed by Burnett et al. (1980) and Burnett & Cooper (1980a,b). This predicts corrections to the Unified theory which take the form of additional correlation terms in the emission coefficients. These terms represent the collisional mixing of l -degenerate levels during far wing emission and are discussed in the context of stellar atmospheres by Cooper et al. (1989). These terms are known to cancel out if the l -degenerate levels are populated according to their statistical weights. It is known that in solar models the l -degenerate levels are populated according to their statistical weights in the chromosphere and so these correlations terms were not included in the study made by Hubeny & Lites (1995). These correlation terms have also been discarded in the present work, but it is noted that, in principle, they may become more significant in the lower gravity stars considered here since the collision rates between the l -degenerate levels will be lower due to the lower chromospheric particle densities. Estimates of the departure from population of l -degenerate levels according to statistical weights have been made and are discussed in Section 4.

3 MODELS

PRD calculations have been performed using atmospheric models of three different stars, the low gravity giant α Tau (K5 III), the higher gravity giant β Gem (K0 III) and the sub-giant Procyon (F5 IV-V). Basic parameters for these stars are given in Table 1.

The α Tau model adopted is that of McMurry (1999). This model was developed from the Kelch et al. (1978) chromospheric model and an observed emission measure distribution for the transition region. It was constructed using an approximate PRD approach, based on a truncation of the Lyman α profile. The properties of the high temperature material in α Tau are not well constrained observationally. The atmospheric model only extends out to a column mass density of $10^{-5} \text{ g cm}^{-2}$ and a temperature $T_e = 10^5 \text{ K}$ which means that the optical depth in both Lyman α and Lyman β is still significant at the top point in the atmosphere. When using this model to predict observations, the atmosphere is extrapolated outwards to zero optical depth, assuming a constant source function. This estimate of the behaviour of the atmosphere above the top of the model lim-

Table 1. Fundamental stellar parameters.

Parameter	α Tau	β Gem	Procyon
Catalogue No.	HD 29139	HD 62509	HD 61421
Spectral Type	K5 III	K0 III	F5 IV-V
T_{eff}	3920 K ^a	4865 K ^e	6500 K ^g
$\log g_*$	1.25 ^b	2.75 ^e	4.00 ^h
Radius	44.3 R_{\odot} ^c	8.93 R_{\odot} ^f	2.1 R_{\odot} ⁱ
Dist. from Sun	19.96 pc ^d	10.3 pc ^d	3.5 pc ⁱ

^a Blackwell, Lynas-Gray & Petford (1991)

^b Bonnell & Bell (1993)

^c Calculated using Blackwell et al. (1991).

^d From Hipparcos (ESA 1997).

^e Drake & Smith (1991)

^f Calculated using Mozurkewich et al. (1991).

^g Ayres et al. (1974)

^h Drake & Laming (1995)

ⁱ Wood et al. (1996)

its the reliability of the calculated line core profiles, up to the wavelength difference from line centre where the optical depth at the top point in the atmosphere becomes negligible, which occurs at a detuning of around 0.4\AA for Lyman α and 0.3\AA for Lyman β . This extrapolation is significant in the calculated integrated line fluxes, particularly the Lyman β CRD flux which is dominated by the flux in the optically thick line core. The α Tau model does not account for the stellar wind which will contain a significant fraction of neutral hydrogen. The wind will introduce an additional source of optical depth above the top of the atmospheric model which further limits the physical reality of the upper boundary conditions in the model. Recent *Far Ultraviolet Spectroscopic Explorer (FUSE)* observations of α Tau will help to constrain the properties of the upper atmosphere of the star.

The β Gem and Procyon models are new and have been constructed by the author in a similar fashion to the α Tau model. The models are based on the chromospheric models of Kelch et al. (1978) and Ayres, Linsky & Shine (1974) respectively, and observed emission measure distributions. These new models are initially constructed using the assumption of CRD. The details of the construction of these models will be discussed in future papers. The new models extend to coronae with $\log T_e = 6.3$. The Lyman lines are optically thin at the top of these coronal models and so the accuracy of the calculated line cores are not limited by an extrapolation in the same way as in α Tau. The electron temperature as a function of the column mass density is shown for each of the models in Figure 1.

4 RESULTS AND DISCUSSION

The Hubeny & Lites version of the MULTI code has been applied to each of the three atmospheric models described in Section 3. Each model has been run for four different cases, the same cases that were studied by Hubeny & Lites (1995), namely:

(a) CRD

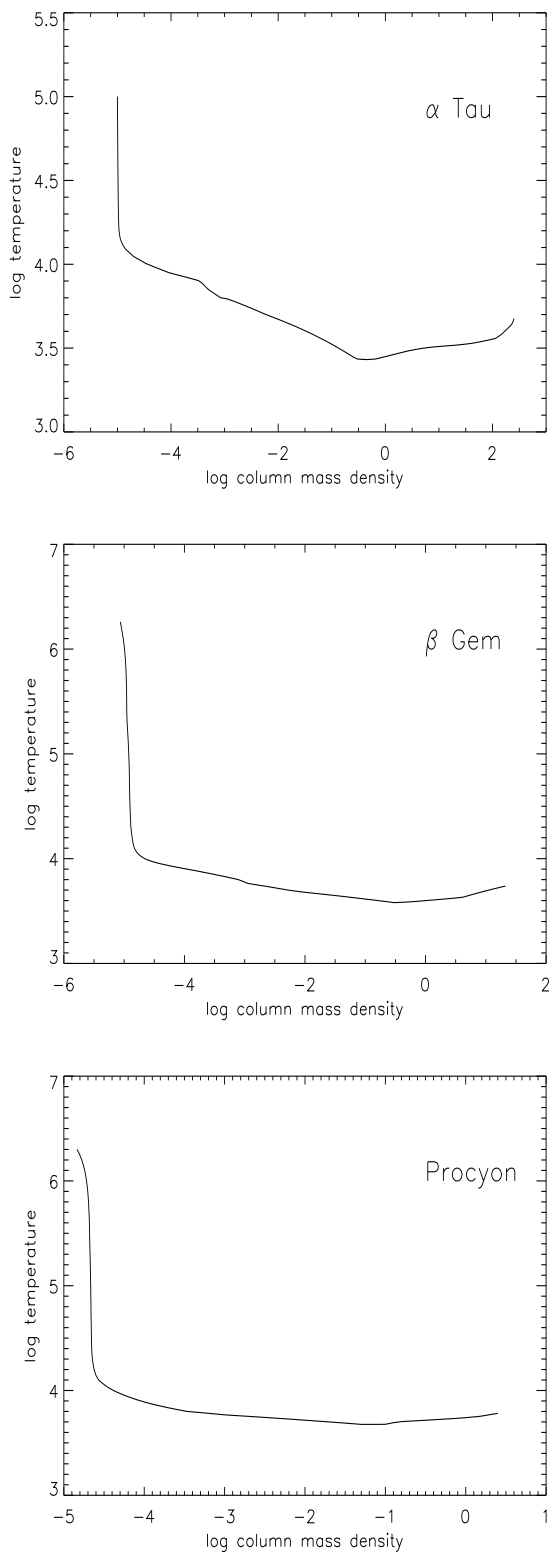


Figure 1. The atmospheric models. In each case the electron temperature is given in K and the column mass density is given in g cm^{-2} .

- (b) PRD resonance scattering in Lyman α ,
- (c) PRD resonance scattering in Lyman α and Lyman β ,
- (d) PRD resonance scattering in Lyman α and Lyman β , and cross-redistribution between Balmer α and Lyman β .

For all twelve of these calculations, the physical depth and frequency dependent coherence fractions were used. Balmer α is treated in CRD throughout (Hubeny & Heinzel 1984 show that PRD is not significant in determining the line profile for a subordinate line, provided that the damping parameters for the upper and lower levels are not too different). The calculations were performed using a nine-level atomic model of hydrogen (the same hydrogen model which was used by McMurry 1999). This model includes 28 bound-bound transitions and 8 free-bound transitions. The Lyman continuum is calculated in detail while the others are treated using radiation temperatures. There is no fine structure in the atomic model (the fine structure splitting between components is much smaller than the width of the Lyman lines and is not observable).

As discussed in Section 2, the PRD treatment employed here neglects certain correlation terms, the importance of which depends upon how closely the l -degenerate levels are populated in accordance with their statistical weights (if the l -degenerate levels are populated exactly according to their statistical weights these correlation terms have no effect). In order to attempt to estimate the relative populations of the l -degenerate levels basic statistical equilibrium calculations have been applied to a simplified fine structure model of hydrogen. This model consists of only six levels (1s, 2s, 2p, 3s, 3p and 3d). The transition rates between these levels due to spontaneous emission, stimulated emission, radiative absorption and electron collisions (both elastic and inelastic) were calculated for an electron temperature $T_e = 10^4\text{K}$ (and the appropriate electron density for each of the three stellar models) using the radiation field from MULTI calculations, the estimates for the elastic collision rates given by Cooper et al. (1989) and the inelastic collision rates calculated by Giovanardi & Palla (1989) (note that while Chang, Avrett & Loeser 1991 show that there are inconsistencies in the rates calculated by Giovanardi & Palla 1989 involving states with $n \geq 4$ they do not find significant problems with the fine structure rates between states with $n \leq 3$). Under the conditions used for each of the three stars it was found that spontaneous emission, radiative absorption and elastic collisions are the important processes while stimulated emission and inelastic collisions are not important under these conditions. The calculated relative level populations for each of the fine structure levels in $n = 2$ and $n = 3$ are given in Table 2. The ratios of statistical weights for the fine structure levels are $\omega_{2p}/\omega_{2s} = 3$, $\omega_{3p}/\omega_{3s} = 3$ and $\omega_{3d}/\omega_{3s} = 5$. The results shown in Table 2 suggest that the fine structure level population ratios are likely to be very close to the ratios of the statistical weights (the greatest variation being 4 per cent in the ratio of the 3d to 3s populations) and so the correlation terms may be safely neglected under conditions typical of the region where PRD effects are important in these stars. When considering these results, it must be borne in mind that the fine structure model that has been used is very simple: transitions between levels with principle quantum number greater than $n = 3$ have been ignored. It is estimated that, for example, radiative decays from $n = 4$

Table 2. Relative level populations for fine structure levels. The notation n_{nl} denotes the population of fine structure level nl .

Star	n_{2p}/n_{2s}	n_{3p}/n_{3s}	n_{3d}/n_{3s}
α Tau	2.97	3.09	4.95
β Gem	2.99	3.03	4.83
Procyon	3.00	3.00	4.94

to $n = 3$ will populate the $n = 3$ at a rate of around ten per cent of the rate at which $n = 3$ is populated by radiative absorption from $n = 2$ (which is the dominant excitation mechanism for $n = 3$ under the conditions in the simple fine structure model).

4.1 Line Profiles

The calculated Lyman α profiles for the four cases of each of the models are shown in Figure 2 and the corresponding Lyman β profiles are shown in Figure 3. These plots confirm that the treatment of redistribution has a significant effect upon the calculated hydrogen line profiles. Most of the differences between PRD and CRD results is due to the effect of coherent scattering (in the atom frame) in Lyman α which is included by PRD but not by CRD. It is clear that the primary effect of a PRD treatment rather than a CRD treatment is a significant reduction in the strength of the Lyman α line wings. This effect occurs because the low incoherence fraction in PRD greatly reduces the number of photons that are scattered into the line wings compared to complete incoherence in a CRD treatment. In all three stars considered, the treatment of Lyman β does not have a significant effect on the Lyman α profile (for each star cases (b), (c) and (d) give identical Lyman α profiles), however the treatment of Lyman α does strongly effect the calculated Lyman β profile. Coherent scattering (in the atom frame) in Lyman α affects the calculated Lyman β as strongly as coherent scattering in Lyman β – coherent scattering in Lyman α traps photons in the Lyman α line which pumps the $n = 2$ level population above its CRD value, this increases the $n = 3$ level population since radiative excitation from $n = 2$ to $n = 3$ (absorption of Balmer α photons) is a significant population process for $n = 3$. This increase in the $n = 3$ population leads to an increased flux in the Lyman β line wings. This effect is evident in all the case (a) Lyman β profiles. The effect of including PRD effects in the treatment of resonant scattering in Lyman β is to reduce the near wing flux by a similar mechanism to that which operates in Lyman α (see above). Finally, the inclusion of cross-redistribution increases the line wing flux again. These effects were all noted and discussed by Hubeny & Lites (1995) for the solar case.

The most striking result from Figures 2 and 3 is the significance of the trend with surface gravity. It is clear that the importance of PRD effects grows rapidly as stars of lower surface gravity (and hence density) are examined. This is to be expected because the elastic collision rates (and hence the incoherence fraction) are smaller in low density stars. As noted in Section 2, PRD is most different from CRD when

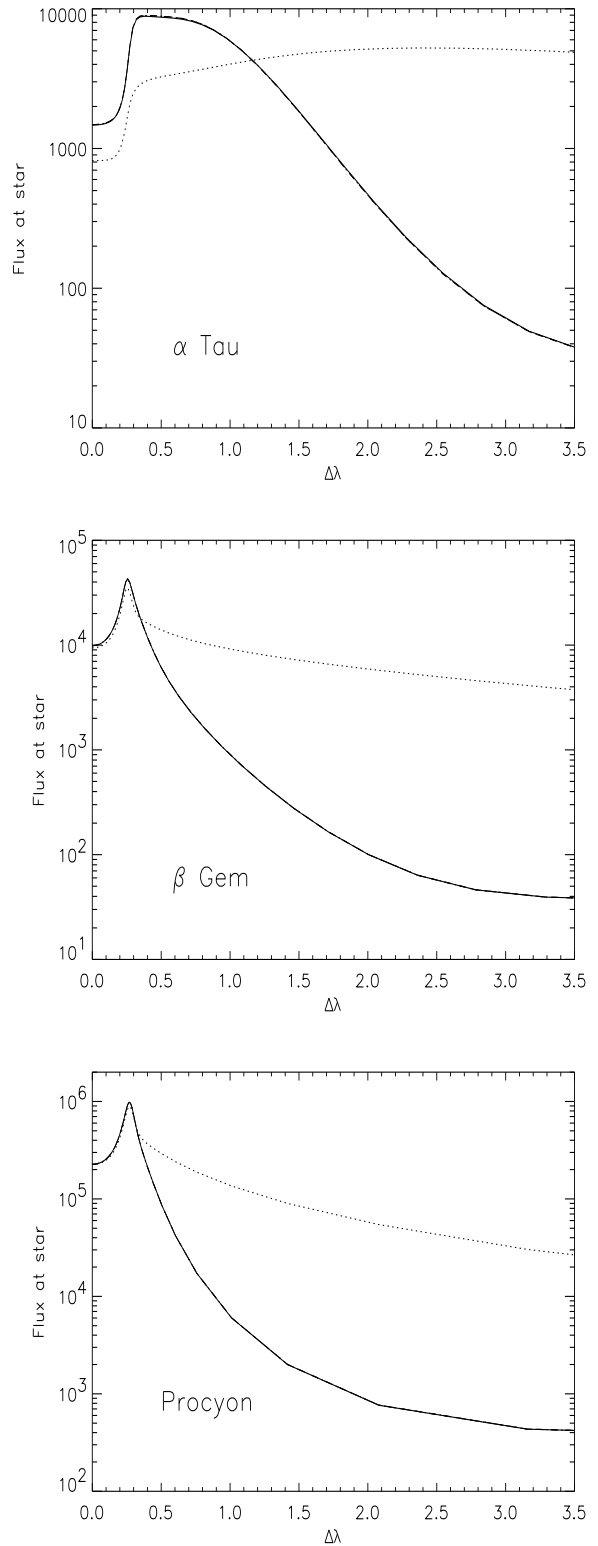


Figure 2. Calculated Lyman α profiles. The dotted line is case (a), the broken line is case (b), the dot-dash line is case (c) and the solid line is case (d) (some cases are indistinguishable: see text). All fluxes are in $\text{ergs cm}^{-2}\text{s}^{-1}\text{\AA}^{-1}$ at the stellar surface. $\Delta\lambda$ is the wavelength relative to line centre in \AA .

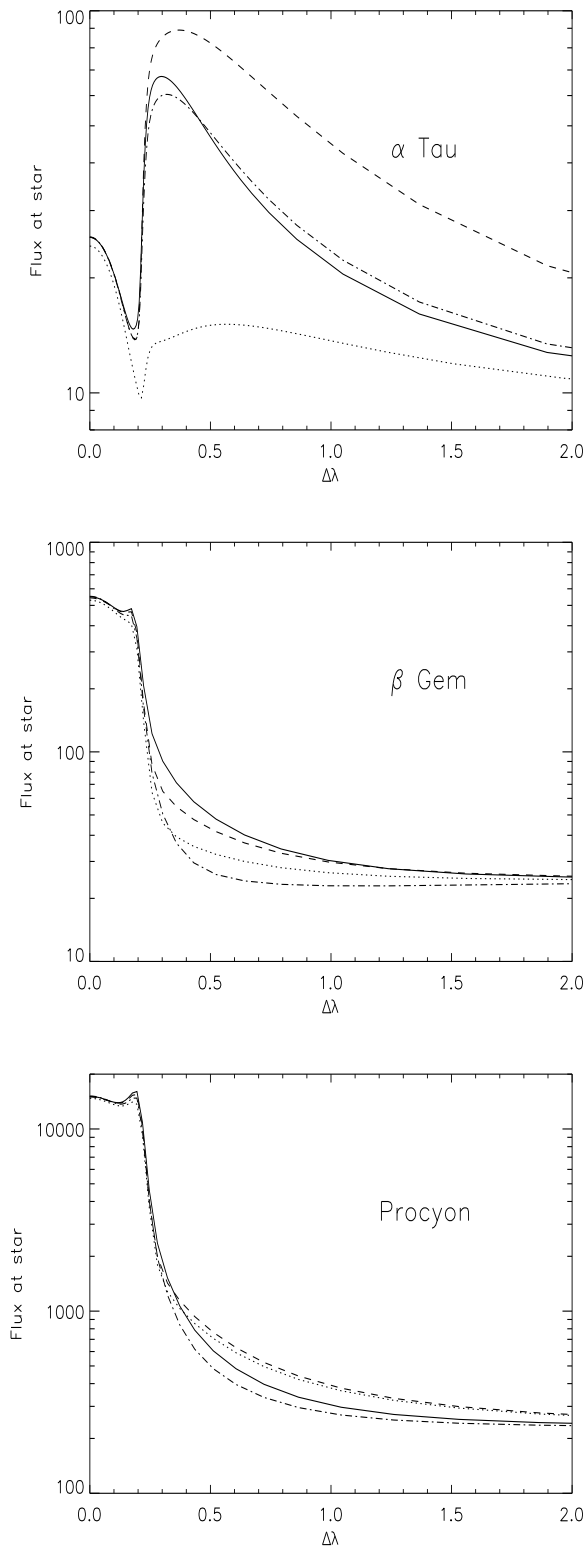


Figure 3. Calculated Lyman β profiles. The dotted line is case (a), the broken line is case (b), the dot-dash line is case (c) and the solid line is case (d). All fluxes are in $\text{ergs cm}^{-2}\text{s}^{-1}\text{\AA}^{-1}$ at the stellar surface. $\Delta\lambda$ is the wavelength relative to line centre in \AA .

the incoherence fraction is small, so it is to be expected that the greatest difference occurs in low surface gravity stars. β Gem and, in particular, α Tau show very much stronger PRD effects than Procyon or the Sun (Hubeny & Lites 1995). In both cases the reduction in the width of the Lyman α line is extremely significant and in α Tau the enhancement of the near wings of Lyman β is sufficient to make them stronger than the line core. Notice that even in these extreme examples of the importance of PRD, its inclusion in the treatment of Lyman β is not as significant as in the treatment of Lyman α . However, the effects on Lyman β are still significant and should not be disregarded.

For comparison the models have also been run in MULTI using two approximate PRD techniques. The first approximate technique (which will be referred to as case (e)) is the commonly used method of simulating PRD effects by performing CRD calculations using a truncated Voigt absorption profile. In the calculations presented here the absorption profiles for both Lyman α and Lyman β have been truncated at $\Delta\lambda = 6\Delta\lambda_D$ where $\Delta\lambda_D$ is the Doppler width (including thermal and microturbulent contributions) at $T_e = 8 \times 10^3 \text{K}$. This form of truncated profile was used by Harper (1992) in the modelling of the ‘hybrid’ giant α TrA and variations on this approximate approach to PRD have been used by many authors (including McMurry 1999 in the modelling of α Tau). The second approximate technique is that suggested by Gayley (1998), which will be referred to as case (f). In that paper, the author suggests that if an approximate PRD method that only requires CRD calculations is required, rather than simply truncating the Voigt profile, one should use a Voigt profile with a depth dependent Voigt parameter, $a_{\text{eff}} = 1.8/\tau$ where τ is the mean optical depth in the line. This approximation is intended to mimic the escape probability for first resonance lines, such as Lyman α , and is not strictly applicable to Lyman β (because of the influence of Balmer α), but it has been applied to both lines for comparison. The profiles calculated using these approximate PRD methods are compared with the case (d) PRD profiles for Lyman α and Lyman β in Figures 4 and 5.

As noted by Gayley (1998), neither of these approximate methods is expected to make accurate predictions for the line profiles and this is evident in Figures 4 and 5. For all six calculated line profiles both the approximate techniques fail to accurately mimic the PRD profile. Owing to the truncation of the absorption profile, case (e) always significantly underpredicts the flux beyond the truncation frequency. For Lyman α , case (f) underpredicts the strength of the inner line wings and overestimates the strength of the outer line wings, producing a profile that is broader than the case (d) profile.

4.2 Integrated Line Fluxes

Table 3 shows the calculated integrated line fluxes at the stellar surface for each of the three models in all six cases considered. These fluxes show that not only the line profile but also the total flux is significantly affected by a PRD treatment; the total flux shows differences of up to a factor of 4.7 between CRD and PRD calculations.

The main application of the approximate PRD techniques is to calculate total line fluxes (as discussed above it is known that they do not predict PRD line profiles cor-

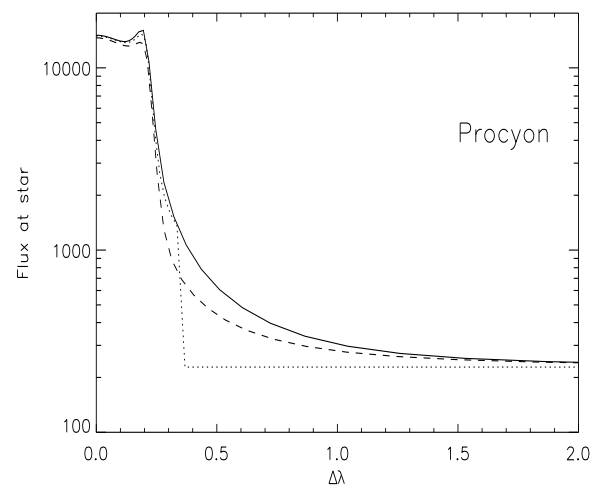
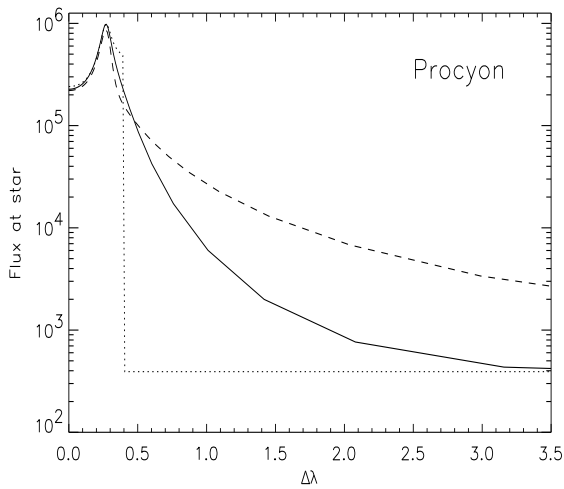
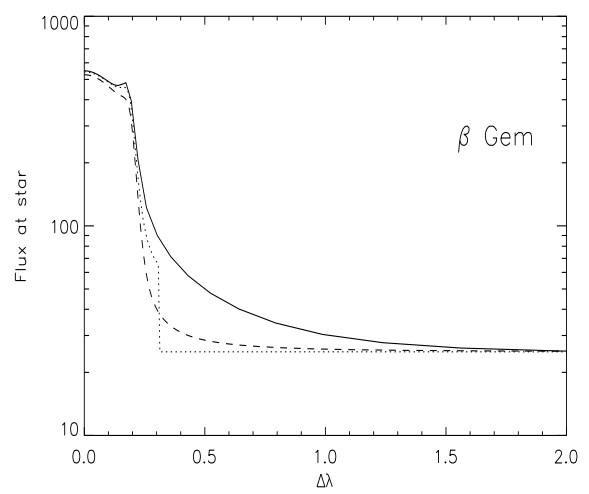
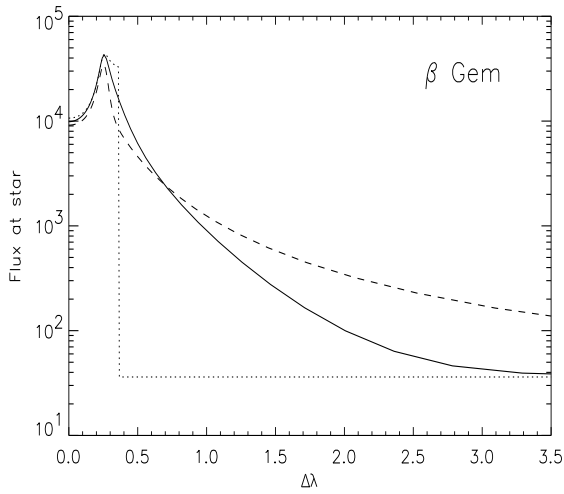
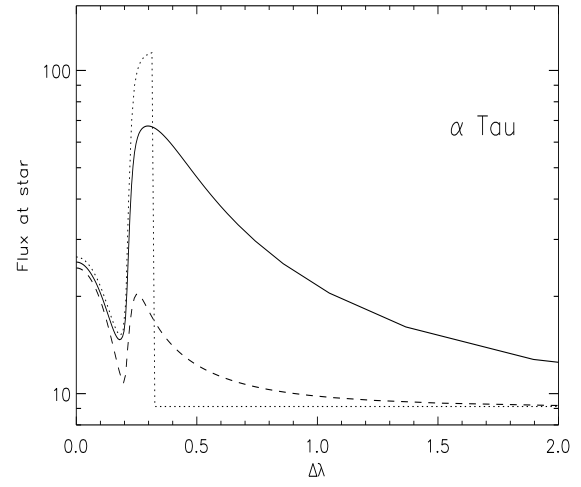
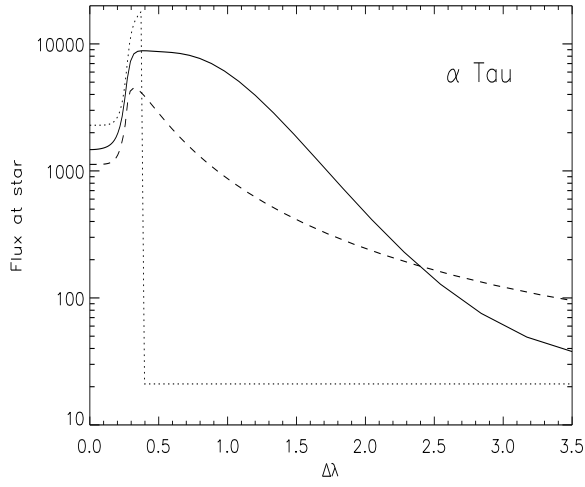


Figure 4. Calculated Lyman α profiles. The solid line is case (d), the dotted line is case (e) and the dashed line is case (f). All fluxes are in $\text{ergs cm}^{-2}\text{s}^{-1}\text{\AA}^{-1}$ at the stellar surface. $\Delta\lambda$ is the wavelength relative to line centre in \AA .

Figure 5. Calculated Lyman β profiles. The solid line is case (d), the dotted line is case (e) and the dashed line is case (f). All fluxes are in $\text{ergs cm}^{-2}\text{s}^{-1}\text{\AA}^{-1}$ at the stellar surface. $\Delta\lambda$ is the wavelength relative to line centre in \AA .

Table 3. Calculated integrated line fluxes from the models. All fluxes are at the stellar surface in $\text{ergs cm}^{-2} \text{ s}^{-1}$.

Line	Case	α Tau	β Gem	Procyon
Lyman α	(a)	8.35×10^4	7.26×10^4	9.67×10^5
	(b)	1.78×10^4	2.06×10^4	4.06×10^5
	(c)	1.78×10^4	2.06×10^4	4.06×10^5
	(d)	1.77×10^4	2.06×10^4	4.07×10^5
	(e)	4.70×10^3	1.69×10^4	3.86×10^5
	(f)	5.67×10^3	1.72×10^4	4.19×10^5
Lyman β	(a)	2.15×10^1	1.99×10^2	7.24×10^3
	(b)	1.54×10^2	2.31×10^2	7.68×10^3
	(c)	7.47×10^1	2.00×10^2	7.12×10^3
	(d)	7.19×10^1	2.48×10^2	7.56×10^3
	(e)	2.36×10^1	2.06×10^2	6.86×10^3
	(f)	9.67×10^0	1.92×10^2	6.65×10^3

rectly). Comparing the PRD integrated line fluxes (case (d)) to those calculated using the approximate methods (cases (e) and (f)) shows that both approximate methods consistently underpredict the integrated line flux (the only exception being Lyman α in Procyon case (f)). The approximate methods work best in Procyon (where the line fluxes agree with the PRD calculations to within 15 per cent) but the discrepancy is larger in the lower gravity stars: in α Tau, case (e) underpredicts the Lyman α flux by a factor of 3.8 and the Lyman β flux by a factor of 3. It is not surprising that these approximate methods, which are based on CRD, work best in Procyon where PRD effects are least important. The fluxes given in Table 3 indicate that for estimating the Lyman α integrated line flux, case (f) is better than case (e), while for estimating the integrated Lyman β flux, case (e) is better (this is not surprising since, as discussed above, case (f) is not appropriate for Lyman β). It is concluded that these approximate techniques can be useful in simulating PRD effects in the higher gravity stars: for Procyon, the case (f) Lyman α flux agrees with case (d) to within 3 per cent and for β Gem, the case (f) Lyman α flux agrees with case (d) to within 20 per cent, compared to a discrepancy between the flux predicted by normal CRD and case (d) PRD of a factor of 2 in Procyon and a factor of 3.5 in β Gem. The approximate techniques appear to be less reliable in the lower gravity star α Tau where case (f) underpredicts the Lyman α flux by a factor of 3.12 and case (e) underpredicts the Lyman β flux by a factor of 3.05. However, as mentioned in Section 3, the significance of the integrated line fluxes in the α Tau model is limited by the reliability of the estimated line core profile produced by the extrapolation of the source function above the top point in the model atmosphere.

Differences between CRD and PRD integrated line fluxes have been shown by Judge (1990) to be related to the line thermalization depth. In that paper the author shows that in a solar model the Mg II k -line (which forms in the chromosphere) thermalizes significantly higher in the chromosphere when using a PRD rather than CRD approach, while in a model of α Tau, the same line thermalizes, for both PRD and CRD calculations, not in the chromosphere but in the photosphere. Because the effective optical thick-

ness of the line depends upon the thermalization depth, this means that the discrepancy between CRD and PRD calculations of the Mg II k integrated line flux is significantly greater in the effectively thick solar model than the effectively thin α Tau model – the more effectively thin the atmosphere the less important are the details of radiative transfer in calculating the emergent flux. Applying the same arguments to Lyman α would suggest that one should expect the discrepancy between computed CRD and PRD line fluxes to be significant only when the atmosphere is effectively thick in Lyman α (i.e. when the Lyman α line thermalizes high in the atmosphere). Figure 6 shows the computed source functions (S) and the Planck function (B) for each of the atmospheric models. The CRD source function is shown along with the monochromatic source function for case (d) PRD at four different wavelength detunings ($\Delta\lambda/\Delta\lambda_D = 0, 6, 18, 35$ where $\Delta\lambda_D$ is the thermal Doppler width at $8 \times 10^3 \text{K}$). It can be seen that thermalization of Lyman α (in the sense that S does not significantly deviate from B) occurs in the chromosphere in each of the models and there is not a strong variation of thermalization depth with surface gravity. This difference between the thermalization properties of Lyman α and the Mg II line is due to the different photon destruction processes which thermalize the lines. In Mg II the line is thermalized by electron collisional de-excitation and since this process occurs at a rate proportional to the electron density the photon destruction rate drops rapidly in the outer atmosphere. This means that the source function can deviate significantly from the Planck function above a certain level in the atmosphere where the electron density has dropped low enough that collisional de-excitation can no longer thermalize the line. Since the value of the electron density is lower in lower gravity stars this decoupling of the source and Planck functions will occur sooner (i.e. deeper in the atmosphere) in lower gravity stars. In Lyman α , collisional de-excitation is a less important thermalization process that photoionization of $n = 2$ by the Balmer continuum. Unlike the collisional de-excitation rate, the photoionization rate does not drop rapidly in the outer atmosphere and so this process is effective in preventing a substantial deviation of S from B until the high chromosphere where the thermodynamic properties of the atmosphere vary sufficiently rapidly that the photoionization process is no longer able to couple S to the local value of B . Thus, Lyman α is not effectively thin in any of the stars considered here and so radiative transfer effects are important in the calculation of both the line profile and the line flux in all the models.

The integrated line flux for Lyman β using CRD agrees with the PRD flux to within 5 per cent for Procyon and 25 per cent for β Gem, significantly closer agreement than was found for Lyman α . In α Tau the difference between CRD and PRD fluxes is somewhat larger (factor of 3.3), but still less than the difference that was found in Lyman α . Figure 7 shows the source functions and Planck function for Lyman β . It can be seen that, like Lyman α , Lyman β thermalizes in the high chromosphere in each of the models and so this line is not effectively thin in any of the models and radiative transfer effects will be important, not only in the calculation of the line profile but also in the calculation of the total flux. The fact that, despite the Lyman β line being effectively thick, PRD and CRD calculations predict line fluxes that agree substantially better than those found for

Lyman α is a strong indication of how much less important PRD effects are in Lyman β than Lyman α , however it must be stressed that the effects of PRD on the Lyman β flux are still significant, particularly in the low gravity stars.

4.3 Implications for Modelling

The calculations discussed above were all carried out using fixed atmospheric models. However, this process is not strictly self-consistent. It is known that using a PRD (rather than CRD) treatment alters the level populations of the hydrogen atom (Hubeny & Lites 1995, Luttermoser & Johnson 1992). Figure 8 shows the level populations calculated for the four different redistribution cases using the β Gem atmospheric model. The variation in the level populations is similar to that found by Hubeny & Lites (1995): the $n = 2$ and $n = 3$ level populations rise because of the increased trapping of photons in the Lyman α line (as described in Section 4.1). An increased $n = 2$ population means that the proton population also rises because the primary ionization mechanism is photoionization from $n = 2$. These increases in the $n = 2$, $n = 3$ and proton populations are balanced by a decrease in the $n = 1$ ground state population. Physically, a significant increase in the proton density carries with it an increase in the electron density and so to hold the electron density constant (at a value calculated from the hydrostatic equilibrium assumption in CRD) is not acceptable. Therefore, it is necessary to use a PRD treatment of hydrogen when constructing a model atmosphere in order that PRD calculation results can be consistent with the assumption of hydrostatic equilibrium.

For this reason, each of the atmospheric models has been recomputed using a PRD treatment of hydrogen in the hydrostatic equilibrium integrations. For α Tau, the original model has simply been recomputed in hydrostatic equilibrium with PRD. This means that the new model of α Tau is no longer strictly consistent with the emission measure distribution from which it was derived by McMurry (1999). The models of β Gem and Procyon have been recomputed in hydrostatic equilibrium with PRD and have also been iterated to consistency with the emission measure distributions from which they were derived. The only difference between the three new PRD-based models and the original three models is in the electron density. Figure 9 shows the change in the electron density in each model. β Gem shows the largest differences, up to a factor of three between the electron density in CRD and PRD calculations. As would be expected, these differences occur in the chromosphere and low transition region, where the Lyman lines are forming. Procyon shows the smallest differences in the electron density of not much more than 20 per cent. α Tau shows significant differences between the CRD and PRD calculations, in a similar way to β Gem, but the maximum change in α Tau is only about a factor of two. It may seem surprising that the lower gravity star α Tau shows smaller changes than β Gem, but it must be borne in mind that the direct comparison of these two models is not valid: the original α Tau model is not a true CRD model but was constructed by McMurry (1999) using an approximate PRD method.

Figure 9 makes clear that a PRD treatment of hydrogen is important in constructing atmospheric models, particularly but not exclusively, for low gravity stars. In, for

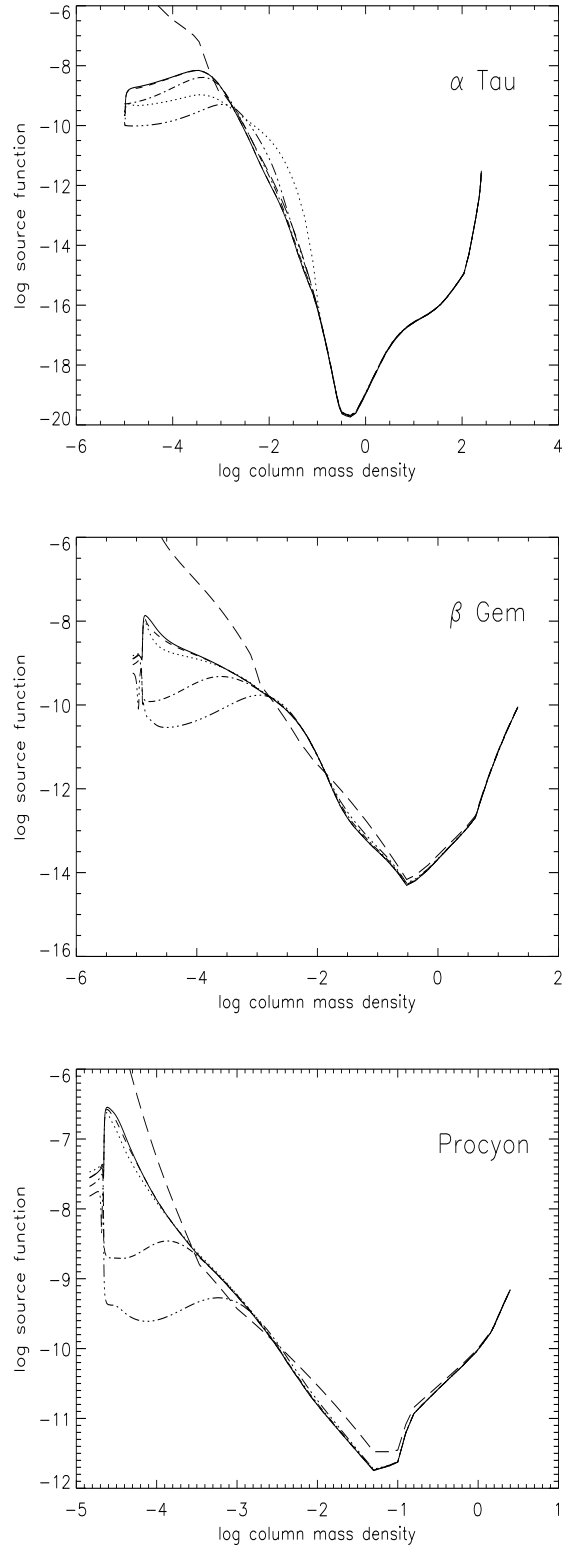


Figure 6. Source functions for Lyman α . In each case the dotted line is for CRD, the solid line is for PRD ($\Delta\lambda = 0$), the dashed line is for PRD ($\Delta\lambda = 6\Delta\lambda_D$), the dash-dot line is for PRD ($\Delta\lambda = 18\Delta\lambda_D$), the dash-triple-dot line is for PRD ($\Delta\lambda = 35\Delta\lambda_D$) and the long-dash line is the Planck function. All source functions are in $\text{ergs cm}^{-2} \text{s}^{-1} \text{sr}^{-1} \text{Hz}^{-1}$ and column mass density is in g cm^{-2} . $\Delta\lambda_D$ is the thermal Doppler width at $T_e = 8 \times 10^3 \text{K}$.

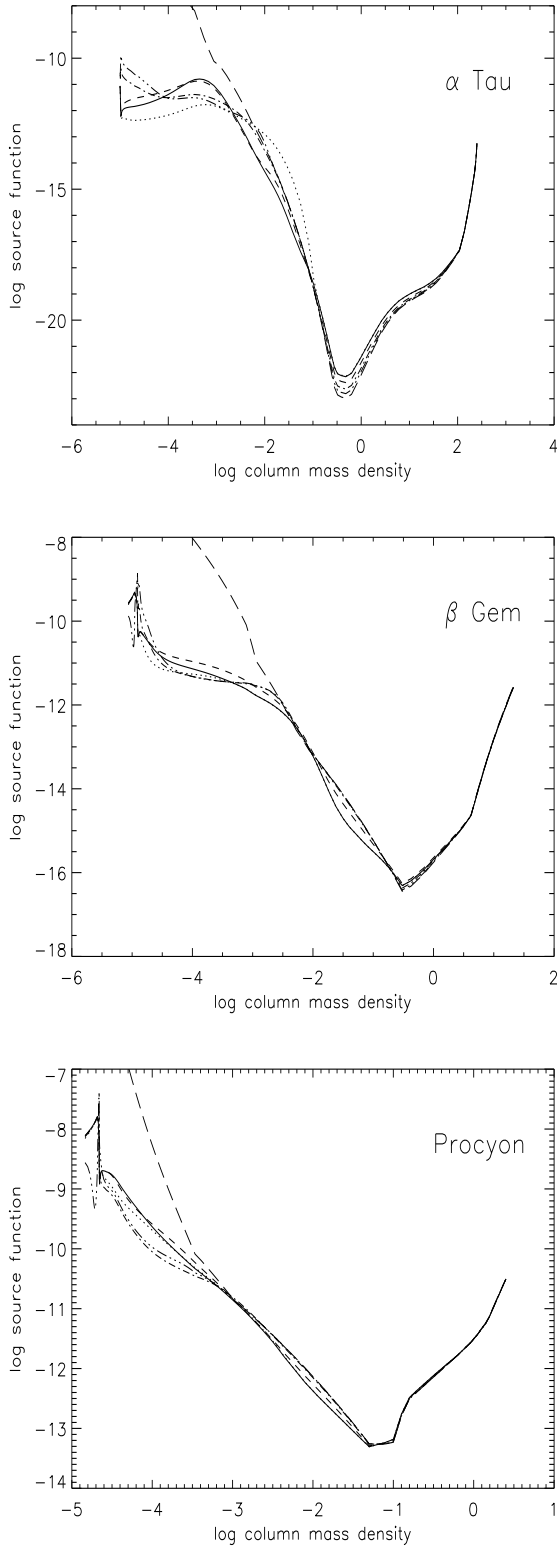


Figure 7. Source functions for Lyman β . In each case the dotted line is for CRD, the solid line is for PRD ($\Delta\lambda = 0$), the dashed line is for PRD ($\Delta\lambda = 6\Delta\lambda_D$), the dash-dot line is for PRD ($\Delta\lambda = 18\Delta\lambda_D$), the dash-triple-dot line is for PRD ($\Delta\lambda = 35\Delta\lambda_D$) and the long-dash line is the Planck function. All source functions are in $\text{ergs cm}^{-2} \text{s}^{-1} \text{sr}^{-1} \text{Hz}^{-1}$ and column mass density is in g cm^{-2} . $\Delta\lambda_D$ is the thermal Doppler width at $T_e = 8 \times 10^3 \text{K}$.

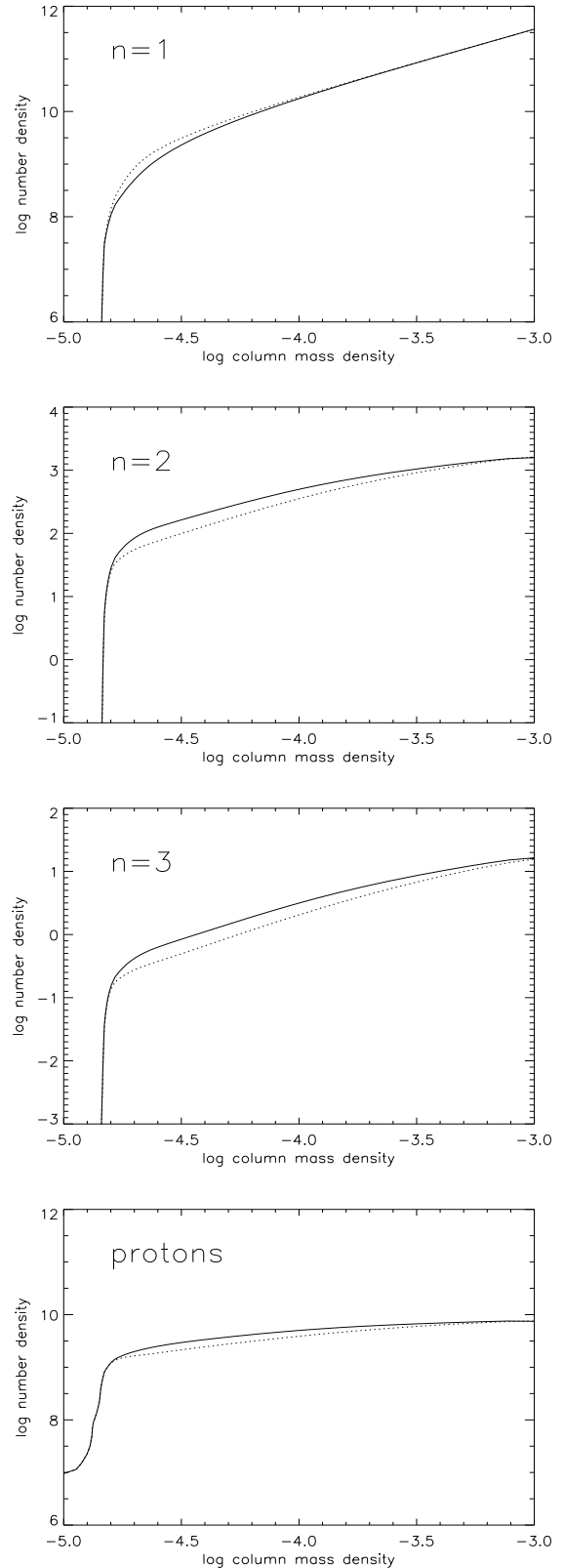


Figure 8. Calculated hydrogen level populations for β Gem. The solid line is case (d) PRD and the dotted line is CRD. Population number densities are in cm^{-3} and column mass density is in g cm^{-2} .

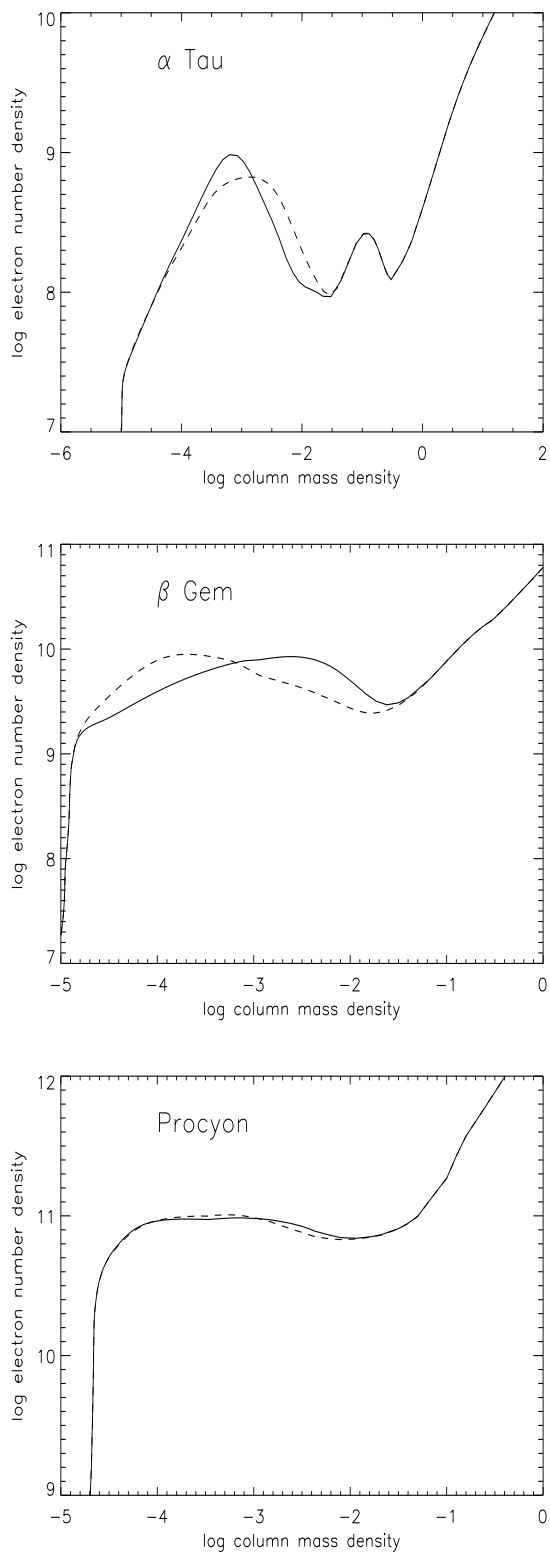


Figure 9. Electron densities from hydrostatic equilibrium calculations. The solid lines are from the original (CRD) models and the broken lines are from models constructed based on hydrostatic equilibrium models computed using a PRD treatment of hydrogen. The electron number density is in cm^{-3} and the column mass density is in g cm^{-2} .

Table 4. Calculated integrated line fluxes from the four new PRD-based models with case (d) PRD treatment of hydrogen. All fluxes are at stellar surface in $\text{ergs cm}^{-2} \text{s}^{-1}$.

Transition	α Tau	β Gem	Procyon
Lyman α	1.23×10^4	3.20×10^4	4.03×10^5
Lyman β	3.79×10^1	3.44×10^2	7.50×10^3

example, the model of β Gem, the electron density in the chromosphere is very significantly different from that predicted by the CRD treatment and it will lead to substantially different fluxes of collisionally excited lines of all elements. It is not within the scope of this paper to give a detailed discussion of the atmospheric emission lines of elements other than hydrogen, but the importance of the PRD treatment of hydrogen on these lines will be discussed in subsequent papers. In particular the collisionally formed lines of C II and the fluorescent lines of O I (pumped by Lyman β) will be of interest. Table 4 gives the integrated fluxes of the Lyman α and Lyman β lines calculated using the full case (d) PRD with the new PRD-based models. If these fluxes are compared with the case (d) results in Table 3 it can be seen that the difference in the fluxes reflects the difference in the electron density: β Gem shows a very significant difference, α Tau shows a significant difference but Procyon shows very little difference.

4.4 Comparison with Observations

The work discussed in the previous sections has led to the conclusion that, for a given atmospheric model, predictions based on a CRD treatment of hydrogen differ from those based on a PRD treatment in three ways. First and foremost, CRD leads to predicted line profiles for Lyman α that have substantially stronger wings (and hence greater integrated line flux) than the more satisfactory PRD treatment. PRD also predicts significantly different profiles for Lyman β in low gravity stars – this effect should be observable in future observations of late-type stars with the *FUSE* instrument. Secondly, because the line profiles are different, there may be differences in the properties of lines that are excited by fluorescence in the Lyman lines, depending on the wavelength at which lines are pumped. Thirdly, because a PRD treatment leads to a different chromospheric electron density there will be a change in the strength of collisionally excited chromospheric/transition region lines (such as the C II lines at around 1335 Å). The secondary effects on the lines of other atomic species will not be discussed here but will be addressed in subsequent papers on the details of the atmospheric models. The most easily observed consequence of PRD (as opposed to CRD) is the significant relative reduction of the line wing intensity in Lyman α compared to the line core. Figure 10 show observed Lyman α profiles and the synthetic profiles calculated using the original models with case (a) CRD, and also the new PRD models treated with full case (d) PRD. The observed profile for α Tau is from the *IUE* high dispersion exposure SWP6679 (C. Jordan (PI)). The observations for Procyon and β Gem are from GHRS

Table 5. Parameters used to correct calculated line profiles for interstellar H I absorption and macroturbulence. For β Gem and Procyon there are two separate components to the interstellar absorption.

Star	Parameter	Value
α Tau	ξ_{macro} (km s $^{-1}$)	17
	ξ_{micro} (km s $^{-1}$)	13
	N_H (cm $^{-2}$)	5×10^{18a}
	b (km s $^{-1}$)	11^b
	v_0 (km s $^{-1}$)	-30^c
β Gem	ξ_{macro} (km s $^{-1}$)	16
	ξ_{micro} (km s $^{-1}$)	12
	N_H (cm $^{-2}$)	$1.15 \times 10^{18}/6.82 \times 10^{17d}$
	b (km s $^{-1}$)	$12.33/11.02^d$
	v_0 (km s $^{-1}$)	$21.9/33.0^d$
Procyon	ξ_{macro} (km s $^{-1}$)	29
	ξ_{micro} (km s $^{-1}$)	14
	N_H (cm $^{-2}$)	$7.5 \times 10^{17}/4.0 \times 10^{17e}$
	b (km s $^{-1}$)	$10.78/10.78^e$
	v_0 (km s $^{-1}$)	$20.5/21.0^e$

^a McClintock et al. (1978)

^b assumed

^c based on Mg II *k*-line (see text)

^d Dring et al. (1997)

^e Linsky et al. (1995)

exposures Z17X0303M (J. Linsky (PI)) and Z2SI0406T (R. Henry (PI)) respectively.

The atmospheric models contain a microturbulent velocity (ξ_{micro}) which is taken into account in the radiative transfer calculations. In order to correctly match the observed widths of optically thin lines, computed profiles generally have to be broadened by convolution with a Gaussian profile whose width corresponds to a most probably macroturbulent speed ξ_{macro} . Macroturbulence is interpreted as large scale turbulence in the stellar atmosphere. The values of ξ_{macro} which have been used are shown (along with the microturbulent velocity ξ_{micro} at $T_e = 10^4\text{K}$) in Table 5. These values of ξ_{macro} have been deduced from the widths of optically thin emission lines that form in similar regions of the atmosphere to the Lyman α line and will be discussed further in later work regarding the atmospheric models. The computed profiles have been corrected for interstellar absorption. This has been performed using the optical depth described by Münch (1968) in terms of the hydrogen column density N_H , the line width parameter b (which in the current work is taken as $\sqrt{2}$ times the Doppler dispersion parameter) and the wavelength shift relative to line centre v_0 . The adopted parameters for the interstellar absorption are shown in Table 5. For Procyon and β Gem, Linsky et al. (1995) and Dring et al. (1997) respectively have deduced parameters for the interstellar absorption using two component models. Both components of the H I absorption have been included here. For α Tau McClintock et al. (1978) give only the column density and so the line width has been taken as a typical value of 11 km s $^{-1}$. The velocity of the interstellar component has been taken to be the same as the velocity of the interstellar absorption component reported in the α Tau

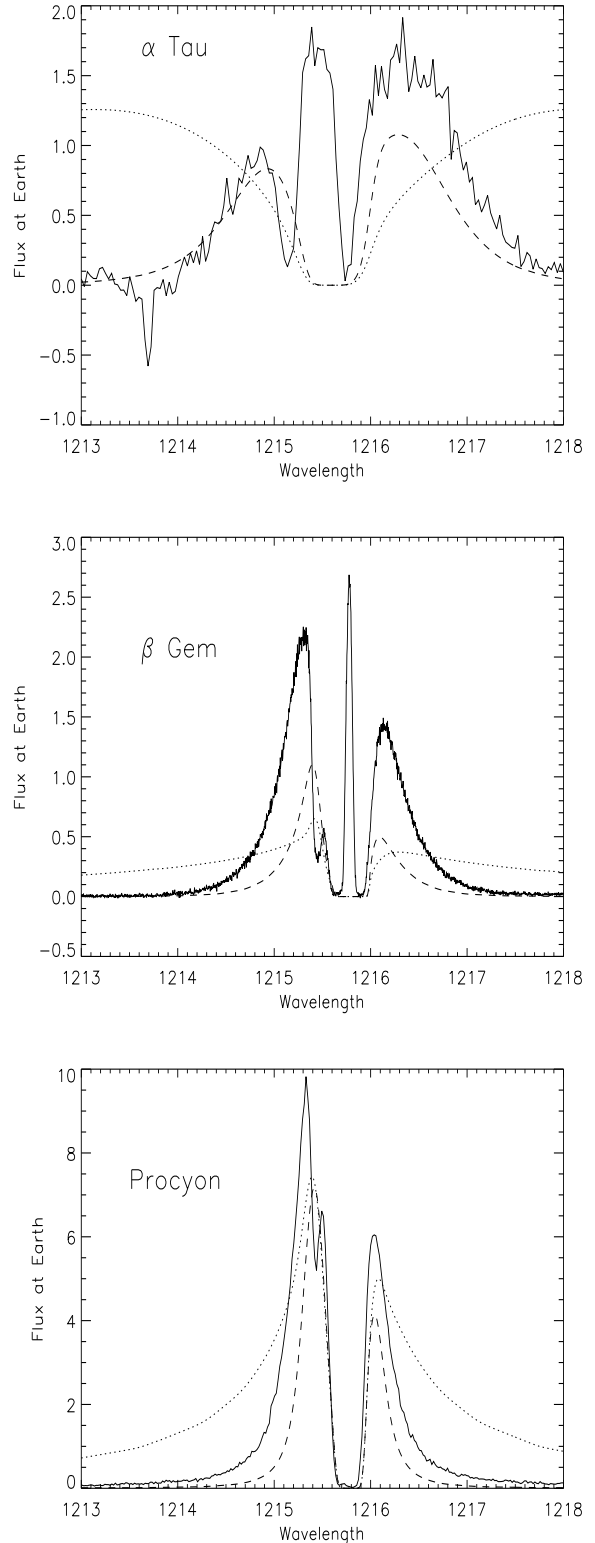


Figure 10. Observed and calculated Lyman α profiles. The solid line is the observed flux, the dotted line is the calculated flux using CRD and the dashed line is the calculated flux using PRD, in units of 10^{-11} ergs cm $^{-2}$ s $^{-1}$ \AA^{-1} . The wavelength is in \AA . The central emission feature in α Tau and β Gem is due to geocoronal emission.

Mg II k -line by Robinson, Carpenter & Brown (1998). For comparison with the observations, the final α Tau profile has been convolved with a Gaussian of FWHM= 25 km s⁻¹ to take the resolution of the *IUE* instrument into account.

It is clear from Figure 10 that the PRD line profiles are in much better agreement with the observed line shapes than are CRD profiles, a clear indication that a PRD treatment is very important to successfully modelling the Lyman α line. The calculated line profiles do not agree closely with the observed profiles, but this is most likely due to inadequacies in the model atmospheres. In particular the total Lyman α flux is being significantly underpredicted in β Gem. It is beyond the scope of this paper to recompute the atmospheric models, but this will be done in future work. The asymmetry of the observed Procyon and β Gem profiles is well accounted for by the effects of interstellar absorption. The significant asymmetry of the α Tau profile is likely to be due to flows in the atmosphere (or stellar wind) which are not included in the hydrostatic model used here. The observed profiles also show additional features due to deuterium absorption (which is seen in the blue wing of the Procyon and β Gem profiles at $\Delta\lambda = -0.3\text{\AA}$ from line center) and geocoronal emission (which is seen as a tall spike near the centre of the β Gem and α Tau profiles).

5 CONCLUSIONS

It has been demonstrated that there are substantial differences between the results of PRD and CRD calculations of the Lyman lines, and that these differences are significant in the modelling of stellar atmospheres. The importance of PRD effects grows in lower surface gravity stars, but the effects are not negligible in any of the evolved stars being studied here. The primary effect has been shown to be a significant reduction in the Lyman α wing intensity which cause a major reduction in the computed Lyman α flux and has significant repercussions on the atmospheric structure because of the way in which it modifies the ionization balance in hydrogen. The differences in Lyman β are less significant and it appears that for lower gravity stars (such as Procyon) this line may be modelled reasonably well with a CRD assumption. However, it has also been demonstrated that this is not always the case: the differences in α Tau are substantial.

The significance of these results goes beyond simply predicting the Lyman line profiles and fluxes. Because Lyman α is such an important radiative energy loss mechanism, its behaviour has repercussions for the understanding of chromospheric heating. The treatment of this line has the power to change the structure deduced for the atmosphere, causing a significant change in the electron density which will manifest itself in the predicted fluxes of collisionally excited emission lines. The issue of fluorescence is also significant and, depending on the wavelength of the pumped lines, the differences between the PRD and CRD profiles could lead to different predicted fluxes of the fluorescent lines. This is important since the lowest gravity stars show the richest spectra of fluorescent lines and it is these stars which show the strongest PRD effects.

The atmospheric models that have been employed as test cases in this paper are preliminary (it is clear from

the comparison in the previous section that they do not, at present, entirely reproduce the observations) but these models provide a useful set of realistic test cases to examine the importance of PRD in hydrogen. The further development and discussion of the atmospheric models will be presented in future work.

ACKNOWLEDGMENTS

I wish to thank C. Jordan for advice and comments during all stages of the work presented here, G. M. Harper for many useful discussions and comments on this manuscript, A. D. McMurry for advice in the construction and use of the atmospheric models, M. Carlsson for helpful discussions and the referee, I. Hubeny, for useful comments and suggestions. I also acknowledge the financial support provided by PPARC (D.Phil studentship).

REFERENCES

- Ayres T. R., Linsky J. L., Shine R. A., 1974, *ApJ*, 192, 93
 Basri G. S., Linsky J. L., Bartoe J-D. F., Brueckner G., Van-Hoosier M. E., 1979, *ApJ*, 230, 924
 Blackwell D. E., Lynas-Gray A. E., Petford A. D., 1991, *A&A*, 245, 567
 Bonnell J. T., Bell, R. A., 1993, *MNRAS*, 264, 319
 Burnett K., Cooper J., 1980a, *Phys. Rev. A*, 22, 2027
 Burnett K., Cooper J., 1980b, *Phys. Rev. A*, 22, 2044
 Burnett K., Cooper J., Ballagh R. J., Smith E. W., 1980, *Phys. Rev. A*, 22, 2005
 Carlsson M., 1986, Uppsala Astronomical Observatory, Report No. 33
 Chang E. S., Avrett E. H., Loeser R., 1991, *A&A*, 247, 580
 Cooper J., Ballagh R. J., Hubeny I., 1989, *ApJ*, 344, 949
 Drake J. J. Laming J. M., 1995, *The Observatory*, 115, 118
 Drake J. J. Smith G., 1991, *MNRAS*, 250, 89
 Dring A. R., Linsky J., Murthy J., Henry R. C., Moos W., Vidal-Madjar A., Audouze J., Landsman W., 1997, *ApJ*, 488, 760
 ESA, 1997, *The Hipparcos and Tycho Catalogues*, ESA SP-1200, Noordwijk
 Gayley K. G., 1998, *ApJ*, 497, 458
 Giovanardi C., Palla F., 1989, *A&AS*, 77, 157
 Harper G. M., 1992, *MNRAS*, 256, 37
 Hubeny I., Heinzel P., 1984, *JQSRT*, 32, 159
 Hubeny I., Lites B. W., 1995, *ApJ*, 455, 376
 Jordan C., Judge P., 1984, *Physica Scripta*, 8, 43
 Judge P. G., 1990, *ApJ*, 348, 279
 Kelch W. L., Linsky J. L., Basri G. S., Chiu H-Y., Chang S-H., Maran S. P., Furenlid I., 1978, *ApJ*, 220, 962
 Linsky J. L., 1985, in Beckman, J., Crivellari, L., eds., *Progress in Stellar Spectral Line Formation Theory*, NATO ASI Series C, Vol 152, p. 1
 Linsky J. L., Diplas A., Wood B. E., Brown A., Ayres T. R., Savage B. D., 1995, *ApJ*, 451, 335
 Luttermoser D. G., Johnson H. R., 1992, *ApJ*, 388, 579
 McClintock W., Henry R. C., Linsky J. L., Moos H. W., 1978, *ApJ*, 225, 465
 McMurry A. D., 1999, *MNRAS*, 302, 37
 McMurry A. D., Jordan C., Carpenter K. G., 1999, *MNRAS*, 302, 48
 Milkey R. W., Mihalas D., 1973, *ApJ*, 185, 709
 Mozurkewich D., Johnston K. J., Simon R. S., Bowers P. F., Gaume R., Hutter D. J., Colavita M. M., Shao M., Pan X. P., 1991, *AJ*, 101, 2207

- Münch G., 1968, in Middlehurst, B., Aller, L., eds., *Nebulae and Interstellar Matter*, Chicago: University Press, p.365
- Omont A., Smith E. W., Cooper J., 1972, *ApJ*, 175, 185
- Robinson, R. D., Carpenter, K. G., Brown, A., 1998, *ApJ*, 503, 396
- Scharmer G. B., Carlsson M., 1985a, in Beckman, J., Crivellari, L., eds., *Progress in Stellar Spectral Line Formation Theory*, NATO ASI Series C, Vol 152, p. 189
- Scharmer G. B., Carlsson M., 1985b, *J. Comput. Phys.*, 59, 56
- Smith E. W., Cooper J., Roszman L. J., 1973, *JQSRT*, 13, 1523
- Smith E. W., Cooper J., Vidal C. R., 1969, *Phys. Rev.*, 185, 140
- Uitenbroek H., 1989, *A&A*, 213, 360
- Vernazza J. E., Avrett E. H., Loeser R., 1973, *ApJ*, 184, 605
- Vernazza J. E., Avrett E. H., Loeser R., 1981, *ApJS*, 45, 635
- Vidal C. R., Cooper J., Smith E. W., 1970, *JQSRT*, 10, 1011
- Wood B. E., Harper G. M., Linsky J. L., Dempsey, R. C., 1996, *ApJ*, 458, 761
- Yelnik J. B., Burnett K., Cooper J., Ballagh R. J., Voslamber D., 1981, *ApJ*, 248, 705